

HIGH TEMPERATURE TREATMENT OF COMPOSITE CEMENT FOR OIL AND GAS WELLS COMPLETION

Gonah, C. M. and Milestone, N. B.

Abstract

The properties of cement can vary in an alarming manner, from manufacturer to manufacturers, even from batch to batch and from any single producer. A small variation in the chemical composition or physical state of cement can cause substantial variations in performance usually in ways that cannot be foreseen. The effect of high temperatures on composite cement systems was studied. Pastes of 100% Ordinary Portland Cement (OPC), 100% Ground Granulated Blast Furnace Slag (GGBFS) and 1:1 OPC/GGBFS were blended at ambient and hydrated at 80°C, 100°C and 140°C for the periods of 1 day, 3 days, 7 days, 28 days and 90 days. The hydration products of the cured samples were characterized by X-ray diffraction (XRD) analysis, differential thermal analysis (DTA) and Scanning Electron Microscopy (SEM). Portlandite [$\text{Ca}(\text{OH})_2$] content of 1:1 GGBFS/OPC was higher at 80°C and lowest at 140°C. Nonetheless, $\text{Ca}(\text{OH})_2$ decreased with the introduction of GGBFS as part replacement of OPC. This implied that part of $\text{Ca}(\text{OH})_2$ was used up in activating the hydration of GGBFS. It is evident from the SEM analysis that elevated hydration temperature enhanced densification. The above characteristics are important if large samples of composite cements are used for oil and Gas wells completion where, the environment is subjected to high pressure and temperature.

Introduction

The most widely used cement is Portland cement. The main minerals in it are alite (C_3S), belite (C_2S), a trisulfate (C_3A) and ferrite (C_4AF). Aluminates are generally the fastest reacting phase in Portland cement. Because the aluminate phase is critical to early hydration properties, it is of great interest in oil wells cementing. Cement reactions are a function of temperature as well as solution concentrations (Taylor, 1997; Malhotra & Mehta, 1996 and Bye, 1999).

In common with many chemical reactions, the hydration of Portland cement compounds is exothermic, typically around 230 - 260 kJ/kg. While for many purposes this heat output can be dissipated easily. When the cement is used in large volumes, such as concrete in dams and vault floors and grouts for containment of wastes and oil wells completion, the temperature rise can be substantial and special efforts need to be conducted to ensure that the heat is evenly spread to avoid cracking due to thermal stresses, hence reducing the useful life of a structure (Bye, 1999; Escalante Garcia & Sharp, 2001; and Escalante et al., 2001).

The temperature at which hydration occurs greatly affects the rate of heat development, which for practical purposes is more important than the total heat produced over a longer period which, can be dissipated to a greater degree with a consequent smaller rise in temperature (Bakharev, Sanjayan & Chang, 1999 and Neville, 2003).

Composite cements based on the partial replacement of Portland cement by waste materials have become common place, because they offer cost reduction, energy saving, adequacy superior products. The replacement materials fall into two principal groups: pozzolanic materials and latent hydraulic materials. The former are pulverized fuel ash (PFA), rice husk ash, volcanic ash and silica fume. Whereas the latter is ground granulated blast furnace slag (GGBFS). In both groups, the replacement materials participate in the hydraulic reactions, contributing significantly to the composition and microstructure of the hydrated product (Civil & Marine Slag Ltd., 2001; Kuennen, 2000 and Hill & Sharp, 2002).

Latent hydraulic materials (GGBFS) have a chemical composition intermediate between that of pozzolanic material and Portland cement. They act as hydraulic cement when mixed with water in the presence of a suitable activator. GGBFS typically has a CaO content of about 40% and can be activated by

alkalis, such as the Portlandite from hydration of alite (Hill & Sharp, 2002; Walker et al., 2001 and Jan, 2002).

Under optimum conditions, which include effective blending of the components and hydration temperature control, these composite cements can have excellent properties, including high ultimate strength, low heat of hydration, low permeability and good durability in a wide range of media. As such, cements containing GGBFS are now well established in the construction industry and oil/gas wells completion (Hill & Sharp, 2001; READYMIX, 2004 and Escalante et al, 2001). However, composite cements with more or less such levels of replacement hydrated at high temperatures are less fully documented, but may have advantages in specific applications, for example when very low heat evolution is required and application of the composite materials is under aggressive temperature and pressure such as oil/gas wells completion.

The aim of the present work was to investigate the effect of high temperatures on phase formation of hydrating composite cement system in 1:1 OP/GGBFS, 100% OPC and 100% GGBFS in a sealed system. Data obtained using X-ray diffraction (XRD) and scanning electron microscopy (SEM), and differential thermal analysis (DTA) to study the hydration products of this composite cement and compared with similar data from controlled samples, based on 100% OPC and 100% GGBFS that were used to make the blended materials; and for possible application in the aggressive high temperatures and pressures zones of oil and gas wells.

Experiment *Materials and Method*

GGBFS and OPC were supplied by the British Nuclear Fuel (BNF) Pic to the department of engineering materials. Escalante-Garcia & Sharp (2001), Escalante et al (2001), Bakharew, Sanjayan and Chang (1999), Hill & Sharp (2001) used mixing method which have been adapted for this research and the 100% GGBFS and the 1:1 OPC/GGBFS because of the absence of OPC and the replacement material respectively. Both the powders were prepared to comply with the specification of modification to the appropriate British standard but with physical and chemical limitations

Casting and Curing

All-samples were prepared with water: sample (w:s) ratio of 0.35. However, this does not equate to a constant water: cement (w:c) ratio of 0.35 for the 100% GGBFS and the 1:1 OPC/GGBFS because of the absence of OPC and the replacement material respectively.

The weighed portions of the distilled water were transferred little by little to the weighed samples while mixing manually with a platinum spatula to obtain a uniform paste. Then, the pastes were carefully poured into polyethyl propylene tubes (centrifuge tubes) until about 90% full. Rocking the tube when full eliminated air spaces.

The samples were cured at 80°C, 100°C and 140°C in a humid environment for 1, 3, 7, 28 and 90 days' period. The cured samples were quenched in acetone to arrest further hydration.

Characterization X-Ray Diffraction

Previously prepared samples were ground by hand in an agate mortar to a fine powder of $63\mu\text{m}$. A Phillips PW1825/00 X-ray diffractometer using monochromatic CuK_α and radiation of 1.540598Å, operating at a voltage of 40kV, current of 30mA was used. A scanning speed of 1°/2G/inh and a step size of 0.02° were used to examine the samples in the range of 5-60° 2θ (Gonah, 2004; Hill & Sharp, 2002 and Brown, 1988).

Scanning Electron **Microscopy**

Cold embedding resin method was used in moulding the samples for SEM. Then samples were polished and coated with gold before SEM was carried out. CAMSCAN microscopy was employed which operated at the voltage of 20kV and magnifications (Gonah, 2004; Hill & Sharp, 2002 and Brown, 1988).

Differential Thermal Analysis

Alumina was used as a reference material. Previously prepared and cured samples were ground to

<60iun. About 25gm of both alumina and samples were put in separate platinum crucibles for the DTA heated from 40°C to 1000°C at the rate of 10°C/min (Gonah, 2004; Hill & Sharp, 2002; Taylor, 1997; and Brown, 1988).

Results X-Ray Traces

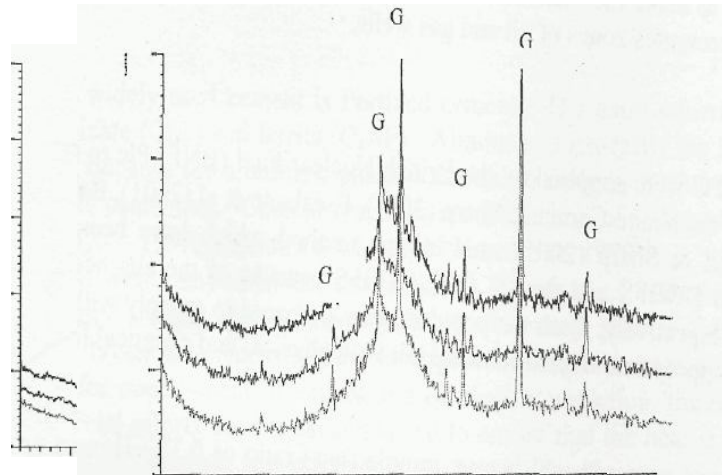


Figure 1: XRD Trace of 100% GGBFS at 28 Days.
Key: Green=80°C, Red=100°C and Blue=140°C, and G=Gehlenite

Figure 2: XRD Traces of 100% OPC at 28 Days
Key: Green=80°C, Red=100°C and Blue=140°C, K = Katoite[Ca₃Al₂(OH)₁₂]

G

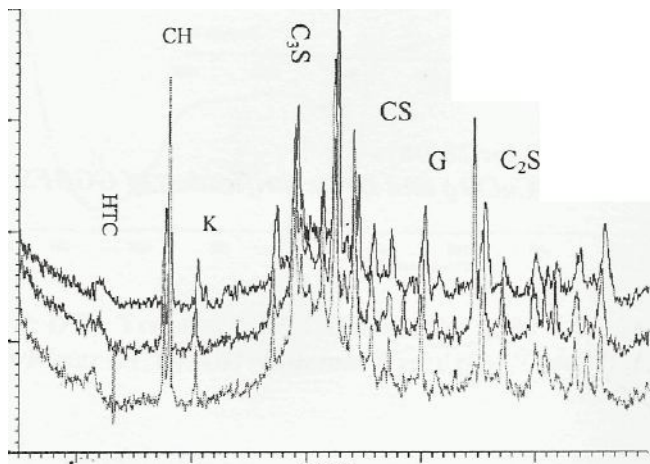
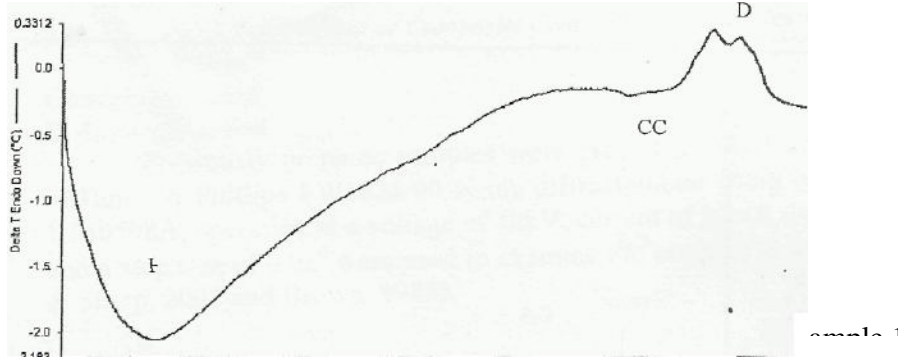


Figure 3: XRD Trace of 1:1 GGBFS/OPC at 28 Days

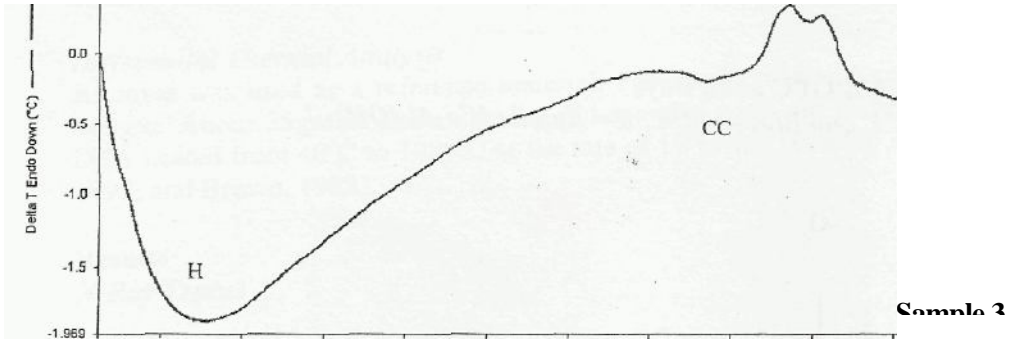
Key: Green=8(fC, Red=100°C and Blue=140°C, K=Katoite/ $\text{Ca}_2\text{Al}_2(\text{OH})_{12}\text{J}$,
 G=Gehlenite(C_2AS) and HTC=Hydrotalctite ($\text{Mg}_6\text{Al}_2(\text{CO}_3)(\text{OH})_6 \cdot 14\text{H}_2\text{O}$)

Differential Thermal Analyses Traces



24.B3 100 500 500 7DO aon son 1000 IDS;
 20D 30Q Temperatu
 400 re (°C)

Figure 4: DTA Trace of 100% GGBFS at 80°C for 28 Days
 Key: H=Water (H_2O), CO Calcium Carbonate (CaCO_3) and D=Devitrification of GGBFS



23.33 100 200 30(400 500 600 700 900
 Temper stute 1D
 (°C) DD
 109
 ;

Figure 5: DTA Trace of 100% GGBFS at 140°C for 28 Days
 Key: H=Water (H_2O), CO Calcium Carbonate (CaCO_3) and D=Devitrification of GGBFS

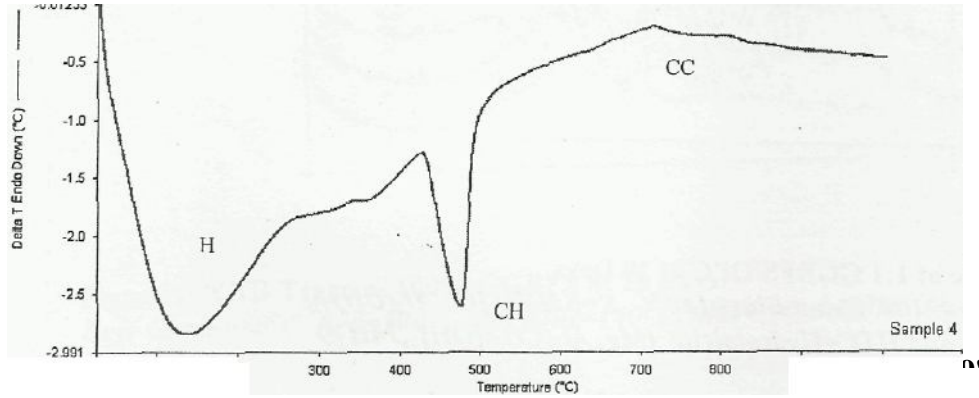


Figure 6: DTA Trace of 100% OPC at 80°C for 28 Days
 Key: H=Water (H_2O), CH=Calcium Hydroxide [$Ca(OH)_2$] and CC=Calcium Carbonate ($CaCO_3$).

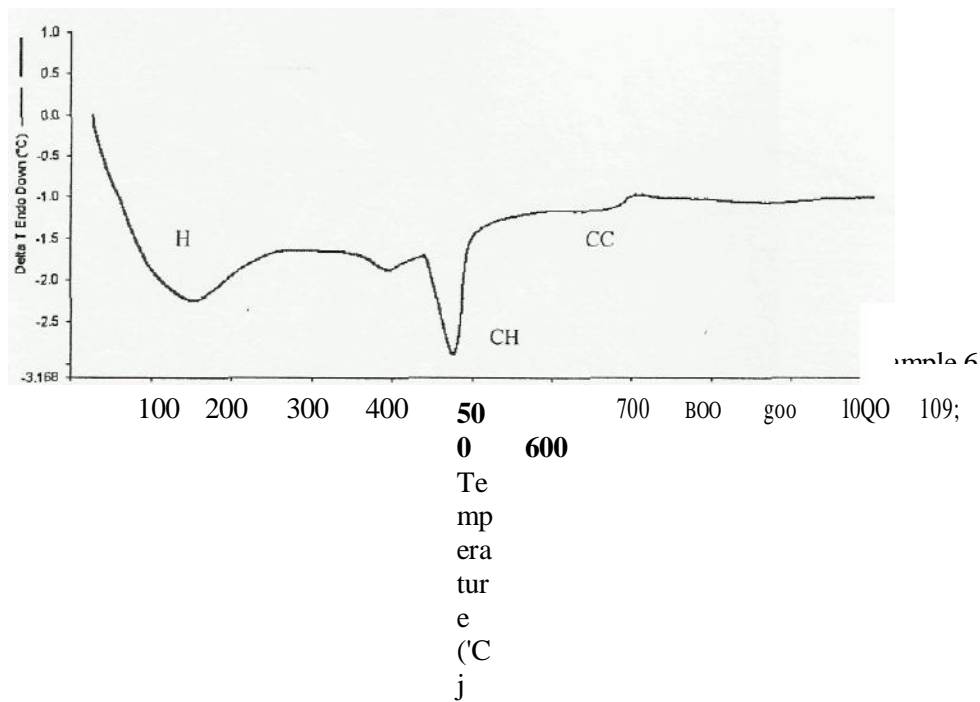
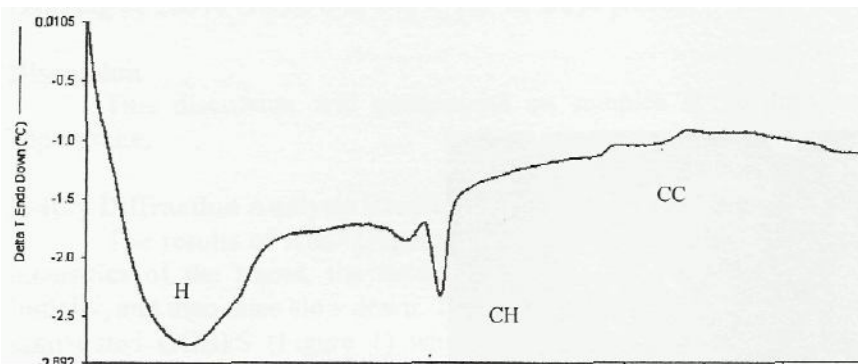


Figure 7: DTA Trace of 100% OPC at 140°C for 28 Days
 Key: H=Water (H_2O), CH=Calcium Hydroxide [$Ca(OH)_2$] and CO=Calcium Carbonate ($CaCO_3$).



Sample 7

24.91	100	300	300	45D		800	900
				O	B00		1000
				Te			1091
				mn			
				eral			
				ur			
				B			
				("C			
)			

Figure 8: DTA Trace of 1:1 GGBFS/OPPC at 80°C for 28 Days

Key: H=Water (H_2O), CH=Calcium Hydroxide [$Ca(OH)_2$] and CC=Calcium Carbonate ($CaCO_3$).

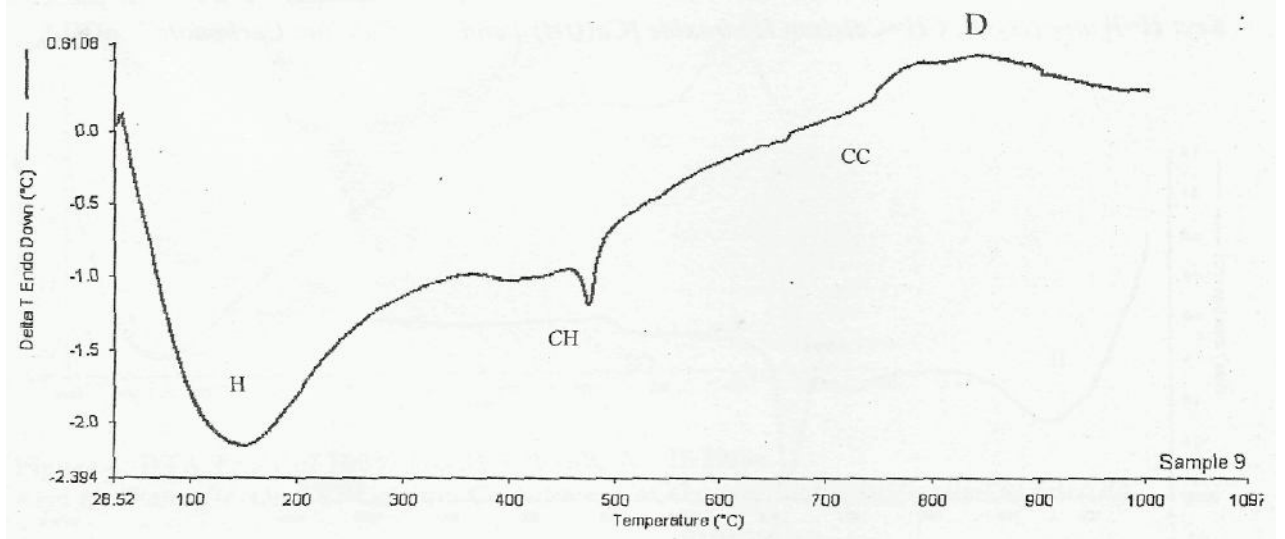


Figure 9: DTA Trace of 1:1 GG15FS/OPC at 140°C for 28 Days

Key: H=Water (H_2O), CH=Calcium Hydroxide [$Ca(OH)_2$], CC=Calcium Carbonate ($CaCO_3$) and D= devitrification of GGBFS

Scanning Electron Images

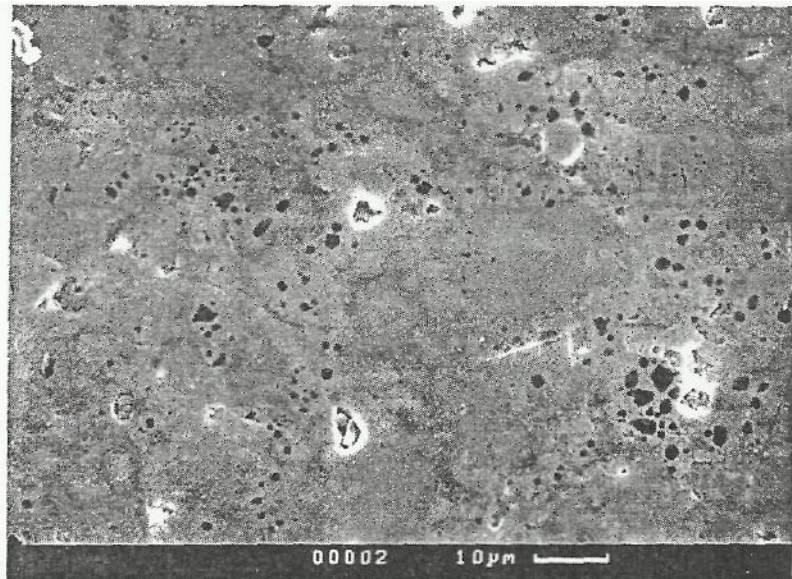


Figure 10: Scanning Electron Microscopy-Back Scatter Imaging of 100% OPC at 140°C for 28 Days X1000.

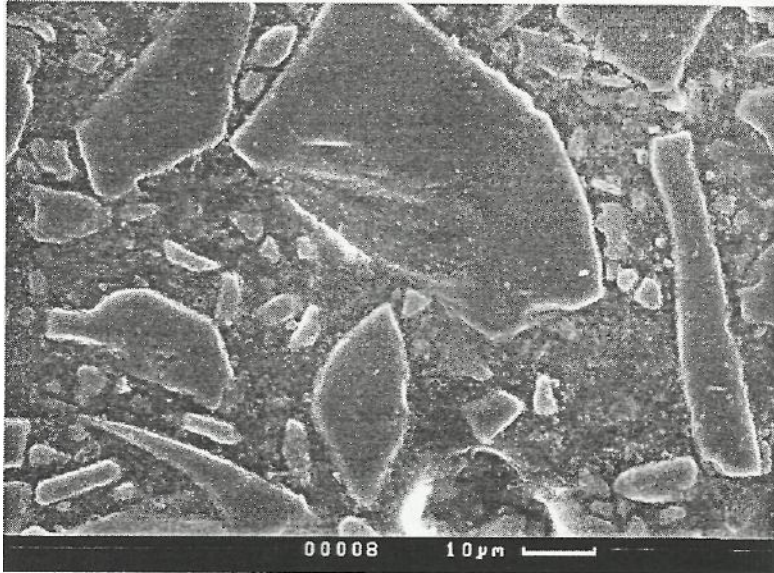


Figure 11: Scanning Electron Microscopy-Back Scatter Imaging of 100% GGBFS at 140°C for 28 Days X1000.

Discussion

This discussion will concentrate on samples at 28 days but will discuss other ages as appropriate.

X-Ray Diffraction Analysis Result at 28 Days

The results of XRD (Figures 1, 2 and 3) indicate that based on a qualitative estimate of the intensities of the traces, the increase in hydration temperature accelerates the rate of hydration initially, and then rates slow down. The period of the initial stage decreases towards 140°C. Unlike the unhydrated GGBFS (Figure 1) whose traces show mainly gehlenite, the 28 days XRD trace of GGBFS in addition to gehlenite shows quartz present resulting from the high silica content of GGBFS. Normally, GGBFS does not set with water even at moderate temperatures unless activated with lime or otherwise. These results show that at 80°C and above, GGBFS is activated thermally and thus hydrated. The alkaline activator opens the silicate structure in the amorphous slag.

On the other hand, the main crystalline phase in OPC (Figure 2) is Ca(OH)_2 which occurs at all three hydration temperatures, even though the peak intensities decrease with decreasing temperatures, and there is more contribution from unhydrated cement. There is little change in traces after 3 days up to 90 days although the amount of unhydrated cement decreases.

Hydrotalcite, Portlandite, katoite, ertringite, and gehlenite were the hydration products found in cement composite 1:1 GGBFS/OPC (Figure 3) at 80°C-140°C, of which CH was highest at 80 °C and lowest at 140 °C. The reduction in CH at higher temperatures is not unconnected to the degree of hydration reaction noted at higher temperatures. The poorly ordered hydrotalcite must have been resulted from MgO usually present in GGBFS and crystallized in the alkaline environment. It has been reported before in GGBFS blends and its disorder may reflect some substitution at the higher temperature. In replacement composites cement, CH decreases with increasing replacement of GGBFS, probably because the GGBFS uses most of it in the reaction.

Differential Thermal Analysis Results at 28 Days

A general pattern of endothermic peaks at the beginning of the DTA thermograms was observed in all the samples at the beginning of the trace. However, with 100% GGBFS (Figures 4 and 5) the valley extends up to about 83 °C. The valleys are endothermic events resulting from

vaporisation or loss of water between 100 °C-200 °C. Interrupted valleys and peaks were observed just before the main endotherm of the water was lost in 100% GGBFS cured at 100 °C, which is believed to be residual acetone that was used to stop hydration reaction.

In the thermograms of the 100% GGBFS samples (Figures 4 and 5) cured at 80 °C, 100°C and 140 °C the exothermic peaks beyond 800 °C signified devitrification of the glassy material presumed to be unhydrated GGBFS . Notwithstanding, endotherms occurred just before the devitrification peaks which are likely to be due to final dehydration, decarbonation, or absorption of heat prior to subsequent crystallization. The glassy phases show two distinct devitrification temperatures which could be formation of akermanite and merwinite devitrifying at 850 °C-900 °C, and intermediate melilites and gehlenite at 930 °C.

100% OPC (Figures 6 and 7) had two endotherms' peaks between 450 °C and 500 °C. The first signified dehydration of $\text{Ca}(\text{OH})_2$ or Portlandite. The three undiluted OPC samples also experience some kind of exothermic peaks which increase with increasing hydration temperatures and could be due to transformations in the calcium silicate phases. Decarbonation is most likely the thermal events.

With: 1 GGBFS/OPC (Figures 8 and 9), the exothermic peak for $\text{Ca}(\text{OH})_2$ reduces with increasing curing temperature, and has almost disappeared in the sample 1:1 GGBFS/OPC at 140 °C. It is clear that much of the Portlandite was used up in activating GGBFS, enhanced by elevated hydration temperatures. The usual exothermic peaks were still present but very small indicating much of the GGBFS has reacted. The pronounced endotherm peak of $\text{Ca}(\text{OH})_2$ in 100% OPC, which reduces as curing temperatures were increased, decreases with increasing GGBFS/OPC ratio as also shown by the XRD results depicting high CH between 15 20 and 18 20 for 100% OPC.

Scanning Electron Microscopy

Backscattered electron images (BEI) from the scanning electron microscopy are presented. They are 100% OPC (Figure 10) cured at 140 °C for 28 days scanned with magnifications of X200, X500 and X1000 per sample. 100% GGBFS also cured at 140 °C for 28 days scanned with X200, X500 and X1000 magnifications per sample.

Features were revealed in the micrographs of the BEI. Images of microstructure of 100% OPC at 80 °C at all magnifications were less dense relative to that of the 100% OPC cured at 140 °C at the same magnifications. In other words, elevated hydration temperature enhances densification. The porosity seen in the micro structure could result from trapped gases but is likely to be due to water. Darker areas show massive $\text{Ca}(\text{OH})_2$ while the lighter patches revealed the unreacted cement. The hydrate is an intermediate grey. No obvious crystals of aC_2SH_3 were seen confirming the XRD results (Figures 1-3).

100% GGBFS (Figure 11) BEI showed large unreacted angular grains held together by much smaller particles of larger surface areas. Even at 28 days it seems to be still amorphous with little or no crystals, and it is less porous relative to 100% OPC.

Conclusion

A pure GGBFS sample hydrated at temperatures up to 140°C does not form crystalline products. However, high temperatures are able to activate the hydration of the slag. In OPC/BFS blends at low temperatures, $\text{Ca}(\text{OH})_2$ is formed initially which activates the hydration of GGBFS. Crystalline phases of katoite and initially $\text{Ca}(\text{OH})_2$ are formed but the amounts are small and the sample retains strength. $\text{Ca}(\text{OH})_2$ is used up in activating the hydration of the slag. This is important if large samples of composite cements are used to encapsulate wastes as the monolith is retained and in oil/gas wells completion in the aggressive temperatures zone. Nonetheless, for specific application in the oil/gas wells completion, further research is imperative to determine setting time and flow-ability for easy pumping of the cement slurry.

References

- Bakharev, T.; Sanjayan J.G.; and Chang, Y. B. (1999). *Effect of Elevated Temperature Curing on Properties of Alkali-activated Slag*, Cem. Cone. Res., 29, 1619-1625.

- Bye, G. C. (1999). *Portland cement-second edition*, Thomas Telford Ltd., Great Britain, ppl-14, 95-126, 163-194.
- Brown, M .E, (1988). *Introduction to Thermal Analysis-Techniques and Applications*. Great Britain: Chapman and Hall, pp 1-49.
- Civil & Marine Slag Cement Limited (2001). *The Effects of Ground Granulated Blast Furnace Slag*, Fact Sheet 3, <http://www.civilmarine.co.uky>. accessed on 30/07/2004.
- Civil & Marine Slag Cement Limited (2004). <http://www.civilmarine.co.uk/>. accessed on 30/07/2004.
- Escalante-Garcia, J.I. and Sharp, J. H. (2001). *Microstructure and Mechanical Properties of Blended Cements Hydrated at Various Temperatures*, Cem. Cone. Res., 31, 195-702.
- Escalante, J. I.; Gomez, L.Y.; Johal, K. K.; Mendoza, G.; Muncha, H.; and Mendez, J. (2001). *Reactivity of Blast Furnaces Slag in Portland Cement Blends Hydrated under Different Conditions*, Cem. Concr. Res. 31, 1403-1409.
- Gonah, C. M. (2004). High Temperature Treatment of Composite Cement Systems. An MSc (Eng) Dissertation, in Ceramics Science and Engineering, Department of Engineering Materials, The University of Sheffield, United Kingdom.
- Hill, J. and Sharp, J. H. (2002). *The Mineralogy and Microstructure of Three Composite Cements with High Replacement Levels*, 24, 191 -199.
- Jan, R. (2002). P.E.P. Cement Americas, *The Birth of the Slag Cement Association*. http://cementmaricas.com/mag/cement_birth_slag_cement/. accessed on 30/07/2004.
- Kuennen, T. (2002). Footings Mark, *Major use of Slag Cement*, Concrete Products. http://concreteproducts.com/mag/concrete_footings_mark_maioir/, accessed on 30/07/2004.
- Malhotra, V. M. and Melita, P. K. (1996). *Advanced in Concrete Technology Volume 1: Pozzolana and Cementitious Materials*, Pub. Gordon and Breach, Canada, ppl-4, 35-67.
- Neville, A. M. f2003). *Properties of Concrete, 4/h-Ed.*, Pearson Prentice Hall, pp 1-56, 62-103, 359-405.
- READYMIX (2004). *Ready Mix Cement Blends, Ready Mix Concrete Incorporating Cement Blends Synopsis*, http://www.rmc.co.uk/crossprQductpages/readymixedconcrete-cement_blends.asp, accessed on 27/06/2004.
- Taylor, H. F. W. (1997). *Cement Chemistry 2nd E&*. Great Britain: Thomas Telford Services Ltd., pp 1-28, 113-156, 187-224,261-293,351-355.
- Walker, P.M.B.; Braithwaite, N. J.; Lewis, P.R.; Reynolds, K. and Weidmann, G. W. (2001). *Chambers Materials Science and Technology Dictionary*. Great Britain: Clays Ltd., pp. 261.